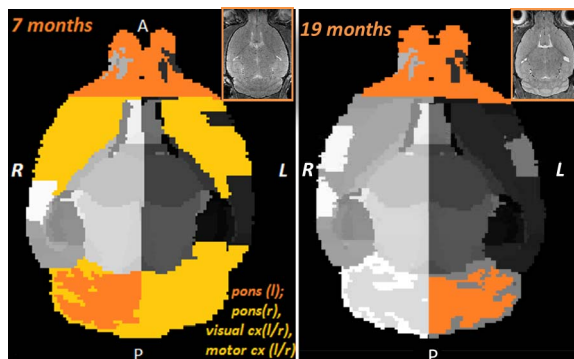


## A Longitudinal Study In Huntington's Disease Reveals Differential Macro- and Micro-structural Effects

Jessica J Stevenon<sup>1,2</sup>, Da Ma<sup>3,4</sup>, Manual J Cardoso<sup>4</sup>, Marc Modat<sup>4</sup>, Mark F Lythgoe<sup>3,4</sup>, Sebastian Ourselin<sup>4</sup>, Rebecca Trueman<sup>2,5</sup>, Anne E Rosser<sup>2</sup>, and Derek K Jones<sup>1</sup>  
<sup>1</sup>Cardiff University Brain Research Imaging Centre (CUBRIC), Cardiff, Wales, United Kingdom, <sup>2</sup>Brain Repair Group, Cardiff University, Cardiff, Wales, United Kingdom, <sup>3</sup>Centre for Advanced Biomedical Imaging (CABI), University College London, London, United Kingdom, <sup>4</sup>Centre for Medical Image Computing (CMIC), University College London, London, United Kingdom, <sup>5</sup>Nottingham University, Nottingham, United Kingdom

**Introduction:** Patient studies in Huntington's Disease (HD) are limited by clinical and genetic variability, and the incompatibility of MRI with chorea, producing an incomplete and inconsistent picture of neuropathological changes across disease stages. Mouse models of HD reduce this variance and enable longitudinal studies across the full span of disease stages. Changes in tissue microstructure are not well understood in HD; diffusion MRI sequences capable of resolving crossing fibers require a lengthy acquisition which limits their application in both patient studies and rodent models, where high spatial resolution is needed to resolve small structures. This study uses both T2-weighted and diffusion MRI (not previously applied in HD mouse models), in a longitudinal design to study tissue macro- and micro- structure at both pre-symptomatic and symptomatic time-points. Despite widespread application to human imaging, automated atlas-based segmentation and diffusion tractography are seldom applied in mice. Here, for the first time, we applied both techniques in a knock-in mouse model of HD and found that macro-structural changes preceded micro-structural changes in the HD brain.

**Method:** 21 HdhQ150 (HD) knock-in male mice and 23 age-matched wild-type (WT) mice underwent *in vivo* MRI on a 9.4T Bruker system at 7 months old, prior to motor symptom onset, and at 19 months old when motor symptoms were evident (n=18; 8 HdhQ150/10 WT). T2-weighted 3-D RARE (120  $\mu\text{m}^3$  resolution, TR/TE = 1750/35 ms, RARE factor = 4, 128 x 128 x 64 matrix) and diffusion MRI (4-shot DTI- EPI; 34 slices 320  $\mu\text{m}$  thick, FOV = 22.4  $\text{mm}^2$ , matrix = 96 x 96, TR/TE=8500/19 ms, 30 DW / 3 B0 directions;  $\delta/\Delta = 4/9\text{ms}$ ,  $b = 1000 \text{ s/mm}^2$ ) were acquired. Pre-processing of the diffusion images involved skull stripping, motion and eddy current correction<sup>1</sup>. Images from the two time-points were co-registered, corrected for partial volume contamination (PVC)<sup>2</sup> and ROI's were drawn manually. Tractography based on constrained spherical deconvolution<sup>3</sup> (CSD, Imax = 6, 0.5mm steps, 40° threshold) was performed and mean tensor-based parameters obtained for the corpus callosum. The T2-weighted images were analysed using an automated multi-atlas based structural parcellation pipeline<sup>4</sup>; images were brain extracted, reoriented into the RAS coordinate, and corrected for intensity non-uniformity. Labels were propagated through non-rigid registration<sup>5</sup> from the NUS atlas<sup>6</sup>, and fused together<sup>7</sup> producing 40 labels per hemisphere (Fig. 1). Volumes were normalised for intracranial volume and statistical analyses were FDR- corrected ( $q=0.05$ ).



**Fig.1.** Volumetric differences pre- (yellow) and post- (orange) normalisation. Cx: cortex, l/r: left/right hemisphere

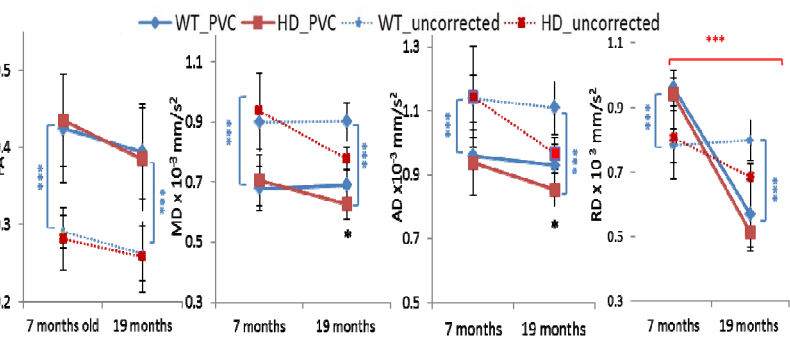


**Fig.2.** Tensor values in the corpus callosum. MD/AD/RD: mean/axial/ radial diffusivity. PVC: partial volume corrected. Error bars=  $\pm 1$  standard deviation. \*\*\* p<0.001, \* p<0.05 FDR-corrected; blue \* = main effect of PVC; red \* = time effect after PVC; black \* = genotype effect after PVC

**Results:** At the 7-month "pre-symptomatic" time-point, reduced volume was found in numerous brain regions (Fig 1) including the caudate-putamen. After normalising for intracranial volume, reduced volume was evident in the olfactory system, left pons, and left cerebellum, whereas there were no differences in microstructure in the corpus callosum. At the 19-month "symptomatic" time-point, in addition to a similar pattern of volume change, differences were seen in microstructure between the HD and WT mice for mean and axial diffusivity values. Radial diffusivity values were reduced in both mouse groups at 19-months compared to 7-months old (Fig 2). Notably, several apparent microstructural effects disappeared after PVC correction (Fig 2, dashed lines).

**Conclusions:** This study advances understanding of the timeline of structural changes in HD, with selective macro-structural changes evident prior to symptom onset and micro-structural changes found in the corpus callosum after symptom onset, suggesting that white matter microstructural abnormalities may be a downstream effect of grey matter abnormalities as opposed to a direct pathogenic mechanism. This study also underpins the importance of correcting for partial volume effects before drawing inferences on tissue microstructure. Despite olfactory dysfunction being reported in HD, this is the first *in vivo* evidence of atrophy in the olfactory system, and fits with *in vitro* evidence of impaired neurogenesis in the olfactory bulb in HD<sup>9</sup>. Specific changes seen in axial diffusivity may implicate axonal processes, however higher-resolution *ex vivo* MRI and immunohistochemistry/electron microscopy analysis are underway to validate and probe the biophysical basis of these results.

**References:** 1. Leemans et al. *ISMRM*. 2009. 2. Pasternak et al. *MRM*. 2009; 62(3):717-30. 3. Tournier et al. *Neuroimage*. 2007; 1; 35:1459. 4. Ma et al. 2012. MICCAI Workshop on Multi-Atlas Labeling. 5. Modat et al. *Comput Methods Programs Biomed*. 2010. 6. Bai et al. *Magn Reson Imaging*. 2012. 30: 789–798. 7. Cardoso et al. *Med Image Anal*. 2013 8. Kohl et al. *BMC Neurosci*. 2010; 11:114. **Acknowledgments:** Wellcome Trust for funding.